Versatile 3D Multi-Sensor Fusion for Lightweight 2D Localization

Patrick Geneva*, Nathaniel Merrill*,
Yulin Yang, Chuchu Chen, Woosik Lee, and Guoquan Huang

Robot Perception and Navigation Group (RPNG)
University of Delaware (UD), Newark, DE, USA

Motivation

- Real-time accurate localization of ground robots
- Large-scale prior map localization
- Use inexpensive sensors:
  - **2D LiDAR, Wheel Odometry, IMU**
- Potential autonomous applications:
  - Warehousing
  - Delivery and service

https://roboticsandautomationnews.com

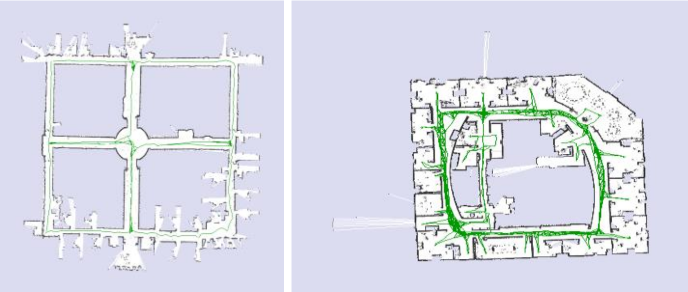

http://ais.informatik.uni-freiburg.de/slamevaluation/datasets.php

Contributions

- 2-stage localization system for robots with inexpensive sensors
  - **2D LiDAR, Wheel Odometry, IMU**
- Stage 1 - Offline occupancy grid mapping
  - Accurate scan matching **uncertainty** modeling
  - **Line tracking** and weighted non-linear batch least-squares for improved map quality in structured environments
- Stage 2 - Online EKF-based prior map localization
  - **6-DoF** filter incorporates IMU to account for true motion of robot
  - Online **spatial-temporal calibration** between sensors to allow for “plug and play”
  - **Light-weight real-time** prior map localization

Related Works

Cartographer [1]

- 2D occupancy grid submaps to enable loop closure detection
- Novel depth-first-search correlative scan matching
- 2-stage scan matching technique
  - Correlative scan for initial
  - Refinement with nonlinear

- **Pose graph is equally weighted (no covariance estimation)**
- **No other geometric features (e.g. lines) used to improve map quality**

HectorSLAM [2]

- Builds a multiple resolution occupancy grid map online
- Fuses 2D LiDAR and IMU
- Estimates a full 6-DoF trajectory

- **No online calibration of sensor extrinsics**
- **Extra cost of building prior map online instead of localizing in known prior frame**

[1] W. Hess, D. Kohler, H. Rapp, and D. Andor, "Real-time loop closure in 2d lidar slam," in 2016 IEEE International Conference on Robotics and Automation. IEEE, 2016, pp. 1271–1278
[2] S. Kohlbrecher, O. Von Stryk, J. Meyer, and U. Klingauf, "A flexible and scalable slam system with full 3d motion estimation," in2011 IEEE International Symposium on Safety, Security, and Rescue Robotics. IEEE, 2011, pp. 155–160.

Stage 1 - 2D Line and Occupancy Grid Mapping

- Create 2D submaps
  - Match to current submap for odometry
  - Keep keyframes as nodes in posegraph
  - Match to old submaps in separate thread (loop closures)
- Accurately estimate scan matching covariance
  - Perform *weighted* batch optimization of constraints
- Extract 2D lines from LiDAR
  - Perform line tracking and mapping

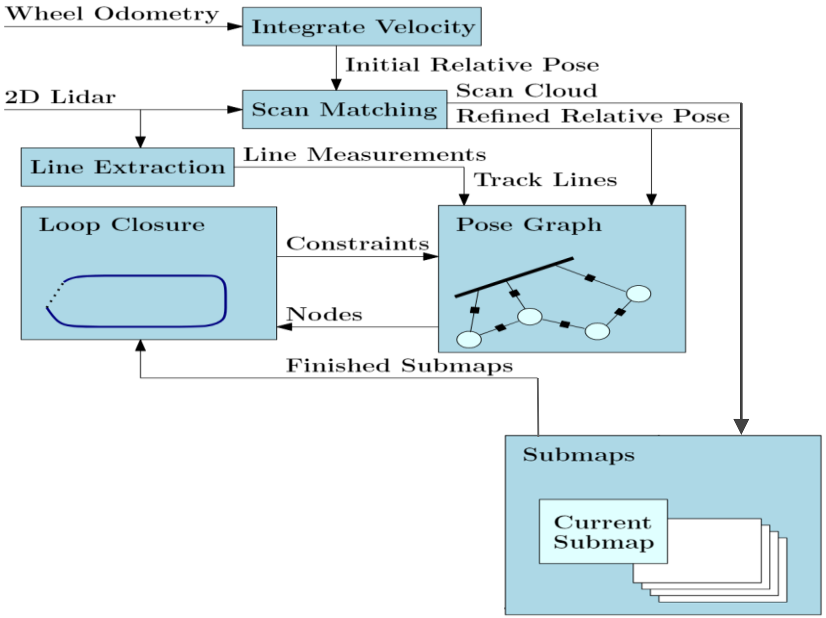

Scan Matching

- Scan matching problem:
  - Optimize the relative LiDAR pose to the submap

$$\underset{^{L_j}\mathbf{x}_{L_k}}{argmin} \left\| \begin{bmatrix} \mathrm{Log}({}^{L_j}_{L_k}\bar{\mathbf{R}}^{\top}\,{}^{L_j}_{L_k}\bar{\mathbf{R}}^{(0)}) \\ {}^{L_j}\bar{\mathbf{p}}_{L_k} - {}^{L_j}\bar{\mathbf{p}}^{(0)}_{L_k} \end{bmatrix} \right\|^2_{\mathbf{\Omega}_{init}} + \sum_{i=1}^{n} \frac{(1 - M_s({}^{S}_{L_k}\bar{\mathbf{T}}({}^{L_k}\bar{\mathbf{p}}_i)))^2}{\sigma^2_{si}}$$

Transformation prior **Occupancy constraints**

- Prior Odometry:
  - Integrated into relative pose
- Prior Scan (accurate to grid res):
  - Exhaustive search or Cartographer's DFS
  - Olson's [3] method for uncertainty

- Covariance
  - Consider noise from scans and from submap occupancy

$$z_i = 1 - M_s({}^{S}_{L_k}\bar{\mathbf{T}}({}^{L_k}\bar{\mathbf{p}}_i - \mathbf{n}_i)) - n_{map}$$

$$\Rightarrow \tilde{z}_i \simeq -\frac{\partial M_s}{\partial {}^{L_j}\tilde{\mathbf{x}}_{L_k}}\,{}^{L_j}\tilde{\mathbf{x}}_{L_k} - \frac{\partial M}{\partial \mathbf{n}_i}\mathbf{n}_i - n_{map}$$

  - Scan uncertainty in residual

$$\sigma^2_{si} = \frac{\partial M_s}{\partial \mathbf{n}_i}\mathbf{Q}_i\left(\frac{\partial M_s}{\partial \mathbf{n}_i}\right)^{\top} + \sigma^2_{map}$$

  - Final scan relative pose information matrix

$$\mathbf{\Omega}_{j,k} = \mathbf{J}_i^{\top}\mathbf{J}_i + \mathbf{\Omega}_{init}, \quad \mathbf{J}_i = \frac{-1}{\sigma_{si}}\frac{\partial M_s}{\partial {}^{L_j}\tilde{\mathbf{x}}_{L_k}}$$

  - Optimized relative pose and information matrix are added as a constraint in pose graph

[3] E. Olson, "Real-time correlative scan matching," in Proc. IEEE Int. Conf. Robotics and Automation (ICRA), 2009

Line Mapping

- Store lines in closest point (CP) [4] format, with the following coordinate transformation from global to LiDAR frame

$$\bar{\mathbf{x}}_f = d \cdot \bar{\mathbf{n}}, \quad \begin{bmatrix} {}^L\bar{\mathbf{n}} \\ {}^L d \end{bmatrix} = \begin{bmatrix} {}^L_G\bar{\mathbf{R}}^\top & \mathbf{0}_{2\times 1} \\ -{}^G\bar{\mathbf{p}}_L^\top & 1 \end{bmatrix} \begin{bmatrix} {}^G\bar{\mathbf{n}} \\ {}^G d \end{bmatrix}$$

- Line Tracking: Lines are tracked by thresholding distance and orientation (normal vector)
- Line Merging: After loop-closure, close lines are merged together with similar thresholding

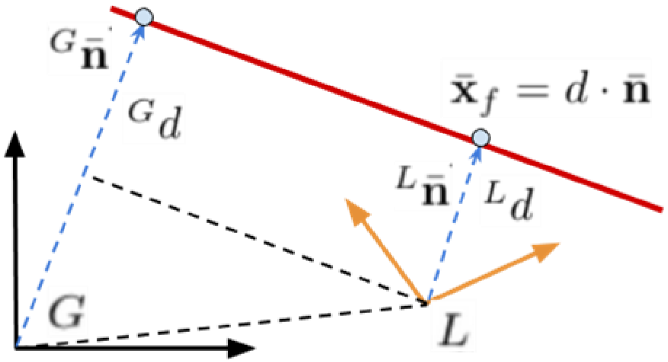

- Lines constrain pose states
  - Multiple states can be constrained with multiple observations of the same line

[4] Y. Yang and G. Huang, “Observability analysis of aided ins with heterogeneous features of points, lines and planes,”IEEE Transactions on Robotics, vol. 35, no. 6, pp. 399–1418, Dec. 2019.

Stage 2 - Online EKF-based Localization

- Estimated states $\mathbf{x}_k = [\mathbf{x}_I \quad \mathbf{x}_L \quad \mathbf{x}_W \quad \boxed{{}^L t_I \quad {}^L t_O}]$ Temporal offset between sensors
  - Inertial: $\mathbf{x}_I = [{}^{I_k}_G\mathbf{R} \quad {}^G\mathbf{p}_{I_k} \quad {}^G\mathbf{v}_{I_k} \quad \mathbf{b}_{\omega_k} \quad \mathbf{b}_{a_k}]$
  - Clones: $\mathbf{x}_L = [{}^{I_k}_G\mathbf{R} \quad {}^G\mathbf{p}_{I_k} \quad {}^{I_{k-1}}_G\mathbf{R} \quad {}^G\mathbf{p}_{I_{k-1}}]$ Historical inertial pose clones
  - Calib: $\mathbf{x}_W = [{}^L_I\mathbf{R} \quad {}^L\mathbf{p}_I \quad {}^O_I\mathbf{R} \quad {}^O\mathbf{p}_I]$ Extrinsic transform of IMU to LiDAR/Wheel sensors
- Measurements:
  - IMU: Angular velocity & linear acceleration (**propagation**)
  - LiDAR: Laser scan distances (in local LiDAR xy plane)
    - **ICP to prior map**
    - **ICP relative to previous frame**
  - Wheel: 2D angular & linear velocity (in global 3D xy plane)
    - **Integrated into relative pose change**

LiDAR Measurement Processing

1. Incoming scan ${}^{L_k}\mathcal{P}$ is "unwarped" with polynomial model to account for motion during collection
2. Local LiDAR frame points are projected to ${}^{L'_k}\mathcal{P}$ in the global xy plane (ensures ICP is performed in same 3D plane)

Projected point global xy plane $\rightarrow$ $\boxed{{}^{L'_k}\bar{\mathbf{p}}_f} = {}^{L}_{I}\bar{\mathbf{R}}\,{}^{I_k}_{G}\bar{\mathbf{R}}\Lambda\left({}^{I_k}_{G}\mathbf{R}^\top\,{}^{L}_{I}\mathbf{R}^\top \boxed{{}^{L_k}\mathbf{p}_f}\right)$ $\leftarrow$ **Point in unwarped scan**

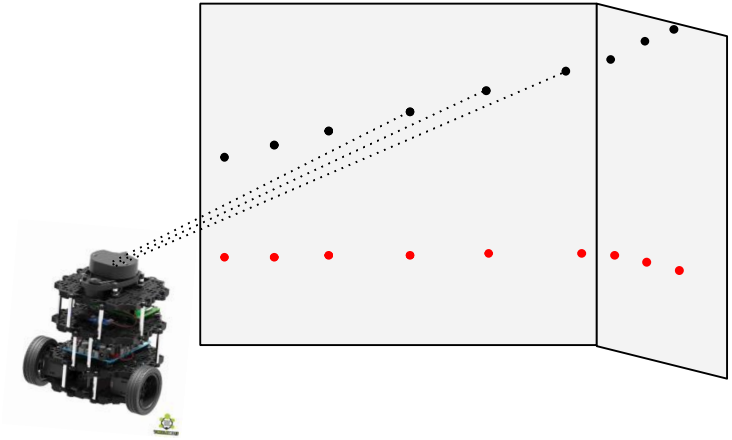

Consistent plane to perform ICP, invariant to sensor roll, pitch

LiDAR Measurement Processing

1. Incoming scan ${}^{L_k}\mathcal{P}$ is "unwarped" with polynomial model to account for motion during collection
2. Local LiDAR frame points are projected to ${}^{L'_k}\mathcal{P}$ in the global xy plane (ensures ICP is performed in same 3D plane)

Projected point global xy plane

$$\boxed{{}^{L'_k}\bar{\mathbf{p}}_f} = {}^{L}_{I}\bar{\mathbf{R}}\,{}^{I_k}_{G}\bar{\mathbf{R}}\boldsymbol{\Lambda}\left({}^{I_k}_{G}\mathbf{R}^\top\,{}^{L}_{I}\mathbf{R}^\top\,\boxed{{}^{L_k}\mathbf{p}_f}\right)$$

Point in unwarped scan

1. ICP is performed relative to the previous scan and global map

$$\left[{}^{L'_{k-1}}_{L'_k}\bar{\mathbf{R}}_m \;,\; {}^{L'_{k-1}}\bar{\mathbf{p}}_{L'_k,m} \;,\; \mathbf{Q}_{icp}\right] = icp\,\boxed{\left({}^{L'_{k-1}}\mathcal{P},\right.}\left.{}^{L'_k}\mathcal{P}\right)$$

Previously received LiDAR scan

$$\left[{}^{L'_k}_{L_k^+}\bar{\mathbf{R}}_m \;,\; {}^{L'_k}\bar{\mathbf{p}}_{L_k^+,m}\; \boxed{, \mathbf{Q}_{icp}\Big]}\right. = icp\left({}^{L'_k}\mathcal{P}, \boxed{{}^{L'_k}\mathcal{M}}\right)$$

Global map (transformed into frame near current)

ICP uncertainty

1. Measurements are rejected based on chi-squared threshold, and relate to state through projected measurement model and time-offset

Wheel Odometry

- From 2D wheel odometry, we generate a "pseudo" 3D measurement

$$
\begin{aligned}
{}^{O_\tau}\boldsymbol{\omega}_m &= {}^{O_\tau}\omega\,\mathbf{e}_3 + \boxed{\mathbf{n}_{\omega\tau}} \\
{}^{O_\tau}\mathbf{v}_m &= {}^{O_\tau}v\,\mathbf{e}_1 + \boxed{\mathbf{n}_{v\tau}}
\end{aligned}
$$

Additional noise to model how close to "planar" odometry is

- Measurements are integrated incrementally between LiDAR times

$$
\begin{aligned}
{}^{O_{k-1}}_{O_{\tau+1}}\mathbf{R} &= {}^{O_{k-1}}_{O_\tau}\mathbf{R}\ \mathrm{Exp}\left(({}^{O_\tau}\boldsymbol{\omega}_m - \mathbf{n}_{\omega\tau})\delta t_\tau\right) \\
{}^{O_{k-1}}\mathbf{p}_{O_{\tau+1}} &= {}^{O_{k-1}}\mathbf{p}_{O_\tau} + {}^{O_{k-1}}_{O_\tau}\mathbf{R}({}^{O_\tau}\mathbf{v}_m - \mathbf{n}_{v\tau})\delta t_\tau \\
\mathbf{Q}_{k-1,\tau+1} &= \mathbf{H}_\tau\mathbf{Q}_{k-1,\tau}\mathbf{H}_\tau^\top + \mathbf{G}_\tau\mathbf{Q}_{m\tau}\mathbf{G}_\tau^\top
\end{aligned}
$$

Measurement uncertainty

- Uncertainty in the timeoffset ${}^{L}t_O$ used to integrate, we model the bounding clone poses as:

$$
\mathbf{z}_{k-1,k} = \begin{bmatrix} \mathrm{Log}({}^{O}_{I}\mathbf{R}\,{}^{I_{k-1}}_{G}\mathbf{R}\,{}^{I_k}_{G}\mathbf{R}^\top\,{}^{O}_{I}\mathbf{R}^\top) \\ {}^{O}_{I}\mathbf{R}\,{}^{I_{k-1}}_{G}\mathbf{R}({}^{G}\mathbf{p}_{O_k} - {}^{G}\mathbf{p}_{O_{k-1}}) \end{bmatrix} + \mathbf{n}_o
$$

$$
\begin{aligned}
{}^{I_k}_{G}\mathbf{R} &= \mathrm{Exp}(-\boldsymbol{\omega}\,{}^{O}\tilde{t}_I)\,\boxed{{}^{I_k}_{G}\hat{\mathbf{R}}} \\
{}^{G}\mathbf{p}_{I_k} &= \boxed{{}^{G}\hat{\mathbf{p}}_{I_k}} + {}^{G}\hat{\mathbf{v}}_{I_k}\,{}^{O}\tilde{t}_I
\end{aligned}
$$

Integrated pose found using best timeoffset estimate

Localization Simulation Validation

- Indoor multi-room office environment (236 planes, 348 meters)
- Simulated realistic sensors and nonholonomic motion
- Prior map simulated based on floorplan

TABLE I: Key simulation parameters for each sensor along with key estimator parameters.

Parameter	Value	Parameter	Value
IMU Freq. (hz)	200	Wheel Freq. (hz)	100
LiDAR Freq. (hz)	10	LiDAR Clones	2
Gyro. White Noise	1.6968e-04	Gyro. Rand. Walk	1.9393e-05
Accel. White Noise	2.0000e-03	Accel. Rand. Walk	3.0000e-03
Odom. Ang. Noise (rad/s)	8.0000e-03	Odom. Vel. Noise (m/s)	2.0000e-02
LiDAR Ray Noise (m)	3.0000e-02	LiDAR FOV (deg)	270
LiDAR Ang. Resolution (deg)	0.5	Prior Map Cell Size (m)	0.05

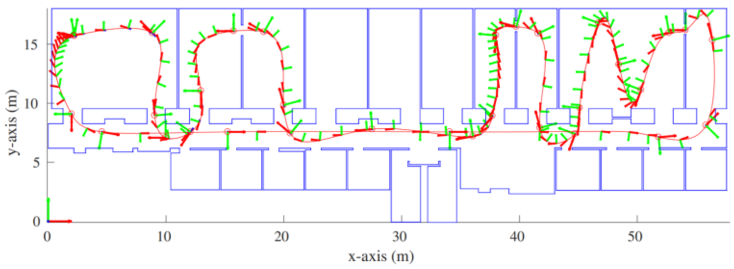

Able to estimate with higher accuracy as more sensors are added. Prior map has the largest impact on reducing error.

Configuration	RMSE Ori. (deg)	RMSE Pos. (m)	NEES Ori.	NEES Pos.
IMU + REL	14.034	4.344	4.122	4.845
IMU + REL + ODOM	3.714	1.221	2.574	1.693
IMU + PRIOR	0.201	0.047	1.979	0.595
IMU + PRIOR + ODOM	0.191	0.043	2.406	1.564
IMU + PRIOR + ODOM + REL	0.182	0.040	2.344	1.464

Prior Map Frequency and Online Calibration

- Frequency of prior map does have small impact on accuracy (robot is moving at 1.8 m/s on average)
- Able to robustly online calibrate sensors.
- Direction normal to the plane of motion not converging as expected

Prior Update Freq. (Hz)	RMSE Ori. (deg)	RMSE Pos. (m)
10	0.182	0.040
1	0.303	0.063
0.20	0.454	0.100
0.10	0.569	0.153

Even 10 seconds between updates (0.10 Hz) we can still achieve < 20cm accuracy

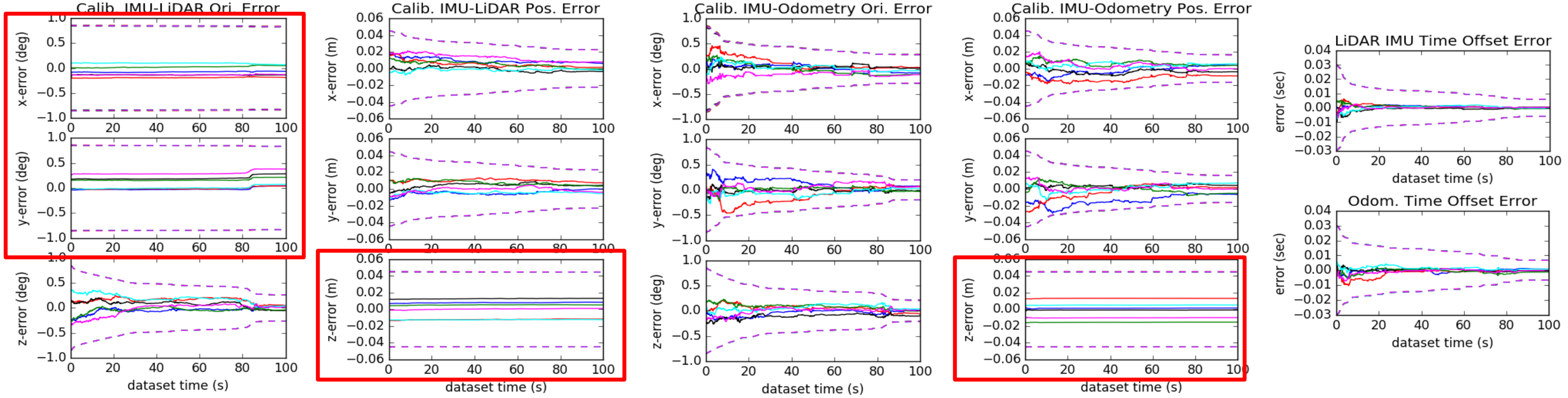

Mapping Accuracy Evaluation

- Evaluated on RADISH datasets comparing to Cartographer [1] and Graph Mapping [5]
- Able to outperform on a number of datasets
- Confirms that **uncertainty** modeling and **lines** improve estimation performance over state-of-the-art

Dataset	Units	Proposed	Cartographer	Graph Mapping
Aces	m deg	$\mathbf{0.013 \pm 0.063}$ $\mathbf{0.081 \pm 0.273}$	0.038 ± 0.043 0.373 ± 0.469	0.044 ± 0.044 0.400 ± 0.400
Intel	m deg	0.046 ± 0.063 $\mathbf{0.274 \pm 1.57}$	$\mathbf{0.023 \pm 0.024}$ 0.453 ± 1.34	0.031 ± 0.026 1.30 ± 4.70
MIT Killian Court	m deg	0.174 ± 0.824 $\mathbf{0.069 \pm 0.339}$	$\mathbf{0.040 \pm 0.049}$ 0.352 ± 0.353	0.050 ± 0.056 0.500 ± 0.500
MIT CSAIL	m deg	0.009 ± 0.034 0.571 ± 4.28	0.032 ± 0.036 0.369 ± 0.365	$\mathbf{0.004 \pm 0.009}$ $\mathbf{0.050 \pm 0.080}$
Freiburg building 79	m deg	$\mathbf{0.012 \pm 0.033}$ $\mathbf{0.153 \pm 1.01}$	0.045 ± 0.035 0.538 ± 0.718	0.056 ± 0.042 0.600 ± 0.600
Freiburg hospital (local)	m deg	0.379 ± 1.94 $\mathbf{0.649 \pm 3.64}$	$\mathbf{0.108 \pm 0.194}$ 0.747 ± 2.05	0.143 ± 0.180 0.900 ± 2.20
Freiburg hospital (global)	m deg	175 ± 420 $\mathbf{1.48 \pm 5.03}$	$\mathbf{5.22 \pm 6.62}$ 3.34 ± 4.80	11.6 ± 11.9 6.30 ± 6.20

[5] G. Grisetti, C. Stachniss, S. Grzonka, and W. Burgard. A tree parameterization for efficiently computing maximum likelihood maps using gradient descent. InProc. of Robotics: Science and Systems (RSS), 2007.

Real-World Turtlebot3 Mapping and Localization

- Demonstration on low-cost Turtlebot3 (separate datasets)
- Two-room and floor-size datasets
- Able to provide continues estimation close to optimized trajectory

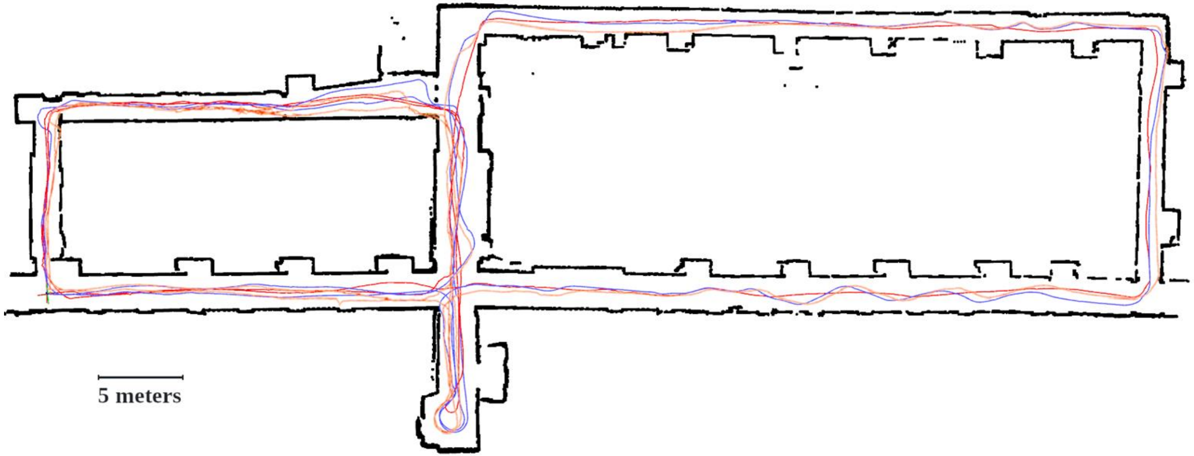

* https://www.turtlebot.com/

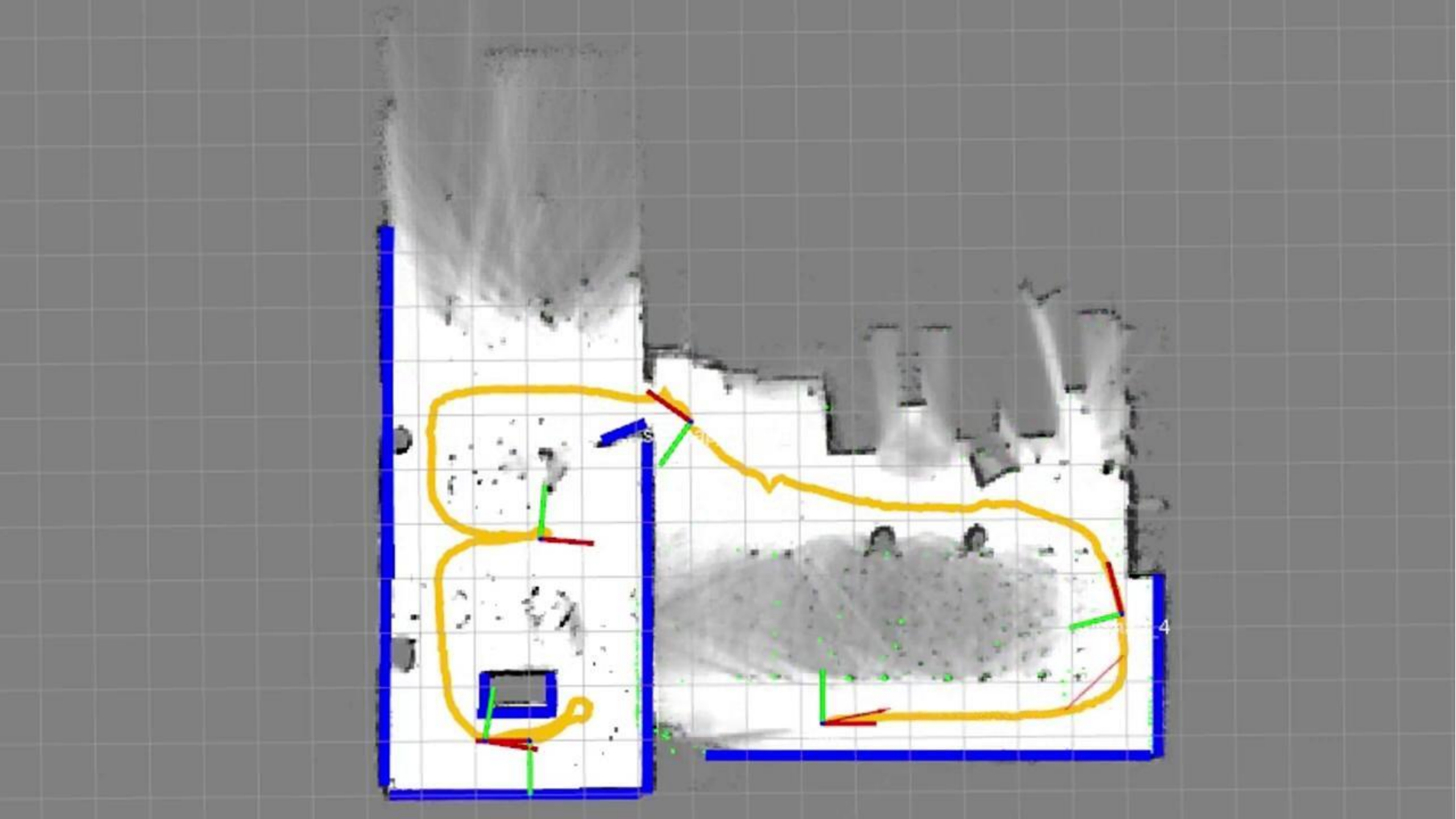
4

Conclusion

- Presented a 2-stage system which first performs accurate **mapping** and then performs efficient **online localization**

- Stage 1 - Prior Map Mapping
  - Improved upon Cartographer, handled **scan matching uncertainty**
  - Improved robustness and accuracy with additional **line features**

- Stage 2 - Online Localization
  - 6-DoF fusion of 2D-LiDAR, IMU, and Wheel odometry with **online calibration** and light-weight **real-time** localization

- Demonstrated performance both in simulation and real-world experiments